Chinese Chemical Letters 33 (2022) 3632–3640

Contents lists available at ScienceDirect

Chinese Chemical Letters

journal homepage: www.elsevier.com/locate/cclet

Working principle and application of photocatalytic optical fibers for the degradation and conversion of gaseous pollutants

Wenhao Xiang[a,1], Jilin Yuan[a,1], Yongwu Wu[a,1], Hongyang Luo[a], Chuanbao Xiao[a], Nianbing Zhong[a,b,*], Mingfu Zhao[a], Dengjie Zhong[c], Yuanyuan He[a]

[a] Intelligent Fiber Sensing Technology of Chongqing Municipal Engineering Research Center of Institutions of Higher Education, Chongqing Key Laboratory of Fiber Optic Sensor and Photodetector, Chongqing University of Technology, Chongqing 400054, China
[b] Liangjiang International College, Chongqing University of Technology, Chongqing 400054, China
[c] School of Mechanical Engineering, Chongqing University of Technology, Chongqing 400054, China

ARTICLE INFO

Article history:
Received 6 July 2021
Revised 27 September 2021
Accepted 24 November 2021
Available online 28 November 2021

Keywords:
Photocatalytic optical fibers
Semiconductor photocatalysts
Gaseous pollutant
Photocatalytic activity
Photocatalytic efficiency

ABSTRACT

Photocatalytic optical fibers are promising for the degradation of gaseous and volatile pollutants in air due to their high specific surface area, high light utilization efficiency, easy regeneration, and sustainability. In particular, photocatalytic optical fibers have proven highly useful for the removal and conversion of different kinds of air pollutants in air. However, these fibers suffer from low photocatalytic degradation efficiencies. In this review, we have focused on introducing photocatalytic quartz optical fibers and photocatalytic plastic optical fibers for the degradation and transformation of gas-phase air pollutants. The principle of photocatalytic optical fibers and main methods for improving their photocatalytic and light utilization efficiencies based on semiconductor photocatalytic coatings are summarized. Moreover, the Langmuir-Hinshelwood kinetic rate equation was summarized to analyze the photocatalytic reduction of gaseous pollutants. Finally, an outlook on the future of photocatalytic optical fibers toward the removal and conversion of gaseous air pollutants is discussed.

1. Introduction

Although modern industries provide support for economic development, they also cause serious environmental pollution, such as the liquid-, gas-, and solid-phase contaminants discharged from human activities and industrial processes [1–4]. Gas-phase contaminants are a problem that must be solved immediately because the increase in air pollution from transportation and petrochemical production has caused an immediate decrease in the clean, fresh air needed to maintain our current and future lives [5]. Recent estimates suggest that exposure to air pollution may be linked to more than 9 million deaths worldwide per year [6], indicating that the contribution of air pollution to global mortality may be increasing. Therefore, it is necessary to improve the air quality by removing or transforming the gaseous contaminants emitted into the air by daily human and industrial activities for the sake of human health.

At present, air pollutant treatment methods mainly include plant adsorption, air fresheners, UV irradiation, ozone, thermal catalysis, electrocatalysis, photocatalysis, *etc.* [7]. Among them, photocatalysis has already been successfully applied for the purification of gaseous pollutants owing to its low energy consumption, environmental friendliness, and sustainability.

The basis of photocatalytic technology is to coat the surface of a substrate such as a lamp casing, glass, polymer, or activated carbon with TiO_2, ZnO, Keggin, or other complex nanostructures that can produce photocatalytically active substances to degrade or convert harmful gas pollutants with light excitation [8–12]. Although promising, there are still many challenges that prevent the practical application of photocatalysis due to the low light utilization efficiencies and mass transmission limitations caused by absorption and scattering of the reaction medium, which makes it difficult to degrade and convert gas contaminants rapidly and efficiently [13].

To solve these problems, Marinangeli and Ollis first proposed the use of optical fibers for both light transmission and as a photocatalyst support because the fibers have low mass transfer resistance for light, and light can emit from the fiber surface to directly excite photocatalytic reactions [14]. Experimental application of this novel idea was demonstrated by Hofstadler *et al.* [15], who

* Corresponding author at: Intelligent Fiber Sensing Technology of Chongqing Municipal Engineering Research Center of Institutions of Higher Education, Chongqing Key Laboratory of Fiber Optic Sensor and Photodetector, Chongqing University of Technology, Chongqing 400054, China.
E-mail address: zhongnianbing@163.com (N. Zhong).
[1] These authors contributed equally to this work.

https://doi.org/10.1016/j.cclet.2021.11.074
1001-8417/

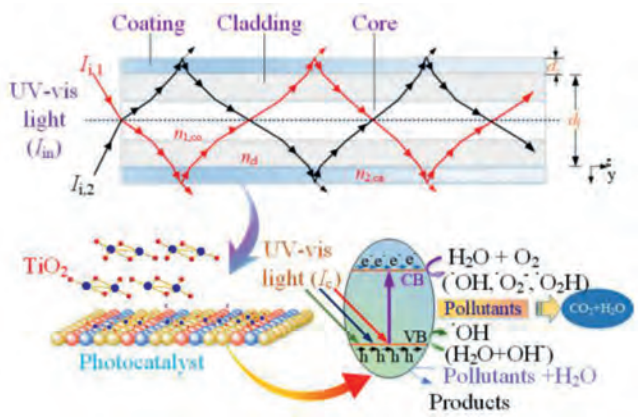

Fig. 1. Illustration of the light transmission and transformation mechanisms of photocatalytic optical fibers toward degrading gaseous pollutants in air. RI: n1 < n2. Abbreviations: CB, conduction band and VB, valence band.

designed a TiO_2-coated quartz fiber for the photodegradation of organic pollutants. Photocatalytic optical fibers have been widely studied as a highly efficient method for the treatment of wastewater, especially the development of TiO_2-coated photocatalytic optical fibers based on quartz optical fibers and plastic optical fibers [4] due to their high specific surface area, high light utilization efficiency, easy regeneration, and sustainability. Thus, numerous photocatalytic optical fibers based on quartz optical fibers and plastic optical fibers as photocatalyst substrates have been reported to degrade and convert pollutants in air [13,16–20]. However, photocatalytic optical fibers face challenges associated with the intensity of light that excites the photocatalyst at the fiber surface, the visible-light response of TiO_2-based coatings, and catalyst poisoning caused by the attachment of photocatalytic byproducts and dust [14,15,21]. These properties of photocatalytic optical fibers in terms of the degradation and conversion of air pollutants have not yet been systematically reviewed.

In this review, we systematically cover the development of photocatalytic optical fibers for the degradation of pollutants in air, with particular focus on developments relevant to photocatalyst-coated quartz and plastic optical fibers. The principles of optical fiber photocatalysis for representative photocatalytic optical fibers and the kinetic equation for the photocatalytic degradation of gaseous pollutants are summarized. We highlight the effects of the optical fiber structural parameters and operation conditions on the photocatalytic and quantum efficiencies reported in the several decades since the first demonstration of pollutant degradation by photocatalytic optical fibers. This information may provide crucial clues toward designing high-performance optical fiber reactors for removing air pollutants. The progress and prospects of photocatalytic optical fibers for the degradation of gaseous air pollutants are finally summarized.

2. Theoretical analysis of fiber-optic catalytic degradation of pollutants

To achieve the photocatalytic degradation and conversion of gaseous air pollutants, a photocatalyst must be fixed on a cladding or thin fiber surface, as shown in Fig. 1. Thus, when the light-incident end of the photocatalytic optical fiber is coupled to a UV-visible light source, the evanescent wave transfers to the photocatalyst coating at the fiber-coating interface because the refractive index (*RI*) of the coating (such as TiO_2) is higher than that of the substrate, such as SiO_2 for quartz optical fibers and polymethylmethacrylate for plastic optical fibers (*RIs* of SiO_2, polymethylmethacrylate, and TiO_2 are 1.548, 1.490, and 2.548, respectively [21]). If the only light exciting the photocatalyst is the evanescent wave at the fiber-coating interface, the light intensity (I_c) of the photocatalyst is dependent on the position along the fiber and can be expressed as Eq. 1 [22]:

$$I_c = \beta_c' I_{in} \exp\left(-\Phi \frac{z}{L} - 2\frac{y}{d_p}\right) \quad (1)$$

where β'_c is the ratio of the light intensity in the photocatalyst to the intensity in the fiber, I_{in} is the incident light intensity in the fiber, Φ is the characteristic decay length for light in the fiber, z is the axial coordinate, L is the length of the photocatalyst-coated optical fiber, y is the radial coordinate into the catalyst from the interface, and d_p is the depth of penetration of the evanescent wave.

The parameter β'_c is a function of the *RI* of the fiber (n_1) and photocatalytic coating (n_2), as well the angle (θ) of the reflecting beam relative to the interface normal (Eq. 2):

$$\beta_c' = \frac{4n_{21}\cos^2\theta}{\sin\theta(1-n_{21}^2)}\left[1 + \frac{2\sin^2\theta - n_{21}^2}{(1+n_{21}^2)\sin^2\theta - n_{21}^2}\right] \quad (2)$$

where $n_{21} = n_2/n_1$. The parameter Φ is determined by the properties of the optical fiber and photocatalytic film and can be expressed as Eq. 3:

$$\Phi = \frac{\alpha_f L}{\sin\theta} + \frac{\beta_f \cot\theta + 4\alpha_c\beta_c d_c}{d_f} L \quad (3)$$

where α_f is the absorption coefficient of the fiber, β_f is the intrinsic surface loss per reflection, α_c is the attenuation coefficient of the TiO_2 layer, β_c is the ratio I_c/I_a for the thin photocatalytic film, I_a is the axial light intensity, d_c is the photocatalytic film thickness, which is below the optimal thickness of the photocatalytic film, and d_f is the fiber diameter.

When an evanescent wave enters the photocatalytic coating, the light can be used by the photocatalyst to generate electron-hole pairs. The generated holes can directly decompose and convert gaseous pollutants and oxidize attached water molecules to form $^{\bullet}OH$, and the injected electrons can then be scavenged by adsorbed oxygen and water molecules to produce advanced oxides ($^{\bullet}O_2^-$, $HO_2^{\bullet-}$, and $^{\bullet}OH$), which can mineralize gaseous organic pollutants into CO_2 and H_2O. According to the simplified model of light intensity and reaction rate constant (r_A) proposed by Wyness *et al.* [23], r_A of a photocatalytic reaction using a photocatalytic optical fiber can be expressed as Eq. 4:

$$r_A = m(I_c)^K \propto \frac{n_1}{n_2}\cdot\frac{1}{\theta}\cdot\frac{1}{d_p}\cdot\frac{d_c}{d_f}\cdot d_c \cdot L \cdot I_{in} \quad (4)$$

where m and K are constants. Eq. 4 shows that the photocatalytic degradation of gas-phase pollutants is similar to the degradation of liquid-phase pollutants [4,21] and that the photocatalytic activity and reaction rate of photocatalytic optical fibers are controlled by their structural parameters (*RI* of fiber core and cladding, fiber diameter, absorption bandwidth of photocatalyst, and coating thickness) and the incident light intensity. Furthermore, the reaction rate is affected by the reaction conditions because the production of $^{\bullet}O_2^-$ and $^{\bullet}OH$ is affected by temperature, pressure, and humidity.

To study the effect of reaction conditions (temperature, pressure, concentration, *etc.*) on photocatalytic reactions for the removal of different types of gas-phase pollutants, the reaction kinetic model based on the Langmuir-Hinshelwood equation has been used to analyze the reaction kinetics, as shown in Eq. 5:

$$r = -\frac{kKC}{1+KC} \quad (5)$$

where k and K are the rate constant and adsorption equilibrium constant, respectively, which depend on the response at ambient temperature, and r is the reaction rate for air pollutant photocatalysis.

3. Degradation of volatile organic compounds using photocatalytic optical fibers

3.1. Degradation of benzene pollutants using photocatalytic optical fibers

Benzene compounds (benzene, toluene, ethylbenzene and xylene) have been identified as strong carcinogens that mainly originate from the volatilization of adhesives, paints, and coatings and exist in the air as vapors [24,25]. Poisoning by benzene compounds generally occurs *via* vapor inhalation or skin contact. Prolonged exposure to excessive amounts of benzene can result in plastic anemia, leukemia, and thrombolysis. In severe cases, exposure can lead to a variety of diseases related to bone marrow suppression, resulting in leukemia, lymphoma, multiple myeloma, or lung cancer. Therefore, the removal of benzene pollutants from the air is crucial.

As a new advanced oxidation technology, optical fiber photocatalysis has been widely used for benzene removal. Photocatalytic quartz optical fibers fabricated with 1.0 mm diameter quartz optical fibers and a TiO_2 photocatalyst coating have been used to degrade benzene pollutants at room temperature [20,26]. In particular, the removal and mineralization of toluene were found to be only slightly inhibited at higher UV intensities near the input side of the fiber [25], revealing that recombination between excess electrons and holes was not critical owing to the adsorption competition between intermediates and toluene on the TiO_2 surface. However, the photocatalytic oxidation of gaseous benzene was shown to be significantly affected by humidity because the water molecules generate hydroxyl radicals, and excess water will compete with the target reactant on the surface of the TiO_2-coated fiber and thus inhibit the photocatalytic reaction [25,27]. Importantly, studies have shown that the deactivated TiO_2-coated fiber can be regenerated by purging with ozone-containing air, indicating that the TiO_2-coated silica optical fibers can be continuously applied to the degradation of benzene pollutants [20,28].

Although TiO_2-coated quartz optical fibers can be used to degrade gas-phase volatile organic compounds, the efficiency for volatile organic compound removal is considerably low because of the limited coating area and low light harvesting ability of the photocatalysts [29]. To enhance the efficiency of quartz optical fibers with a TiO_2-based coating for the degradation of gaseous 1,2-dichlorobenzene, macroporous photonic bandgap TiO_2 with an inverse opal topology was fabricated and coated on the optical fibers using polystyrene templates and sol-gel chemistry [29]. The photocatalytic efficiency of the optical fiber with the photonic bandgap TiO_2 coating at a thickness of 3 μm was enhanced because of the increased "slow photon" intensity on the red edge of the photon bandgap and reduced light scattering associated with the regularity of the photonic titania pore structure [30]. These factors improved the light transmission capability of the photocatalytic fiber and enhanced the photon utilization efficiency of TiO_2.

A sunlight-/visible-light-responsive photocatalyst, *i.e.*, graphitic carbon nitride with a suitable bandgap, has also been developed, and $H_3PW_{12}O_{40}$/graphitic carbon nitride film-coated optical fibers (fiber length of 8 cm, fiber diameter of 600 μm, and $H_3PW_{12}O_{40}$/g-C_3N_4 coating thickness of 8 μm) were prepared *via* a sol-gel-dip-withdrawing route [31]. The $H_3PW_{12}O_{40}$/graphitic carbon nitride-coated optical fiber photoreactor, which is shown in Fig. 2, exhibited enhanced gas-phase photocatalytic removal efficiencies for benzene, toluene, and *m*-xylene at a relative humidity of 73% in an air atmosphere [32]. The well-matched energy band structures and intimate contact of the Keggin unit structures and graphitic carbon nitride accelerated interfacial charge carrier separation and led to plentiful $^{\bullet}O_2^-$ and $^{\bullet}OH$ radicals involved in the reactions, which enhanced the photocatalytic activity. In addition, the increased contact area between the catalyst film and quartz optical fiber and the improved light harvesting capability also promoted the activity of the $H_3PW_{12}O_{40}$ graphitic carbon nitride film.

3.2. Degradation of acetone and isopropanol using photocatalytic optical fibers

The volatile organic compounds acetone and isopropanol in petrochemical products can trigger acute poisoning, causing severe damage to human organs and the nervous system. Therefore, the treatment of gas-phase isopropanol and acetone contaminants has attracted extensive attention. Photocatalytic reactors using photocatalytic semiconductors combined with optical fibers have been used for the degradation and conversion of gaseous acetone and isopropanol pollutants. However, the environmental humidity and light energy limitations affect the performance of such fiber-optic photocatalytic reactors. As shown in Fig. 3a, photocatalytic fiber bundles with a 1.5 μm thick TiO_2 coating were used to mineralize acetone in air [33,34]. The results showed that the formation of hydroxyl radicals ($^{\bullet}OH$) on the surface of the TiO_2-coated quartz optical fibers can be increased by increasing the humidity appropriately, which promotes the photocatalytic reaction under UV light. However, the photocatalytic conversion efficiency of the TiO_2-coated quartz optical fibers was negatively affected by the competition between water and acetone molecules for the active centers on the surface. Additionally, the conversion of acetone to CO_2 increased synchronously with the incident light intensity without showing any signs of saturation during acetone gas-phase degradation. This indicates that the photocatalytic activity of photocatalytic optical fibers is affected by the intensity of the light exciting the TiO_2 coating, since absorption by TiO_2 causes the intensity of the propagating light to exponentially decrease along the length of the coated fiber [14,22,33].

To address the light constraints and maintain a high quantum efficiency, as shown in Fig. 3b, photocatalytic quartz optical fiber bundles (18,000 pieces, 125 μm diameter) coated with TiO_2 layers (2 μm thick) were used for gas-phase isopropanol degradation under 365 nm UV light (input light intensity 1.6×10^{16} quanta cm^{-2} s^{-1} to 2.6×10^{17} quanta cm^{-2} s^{-1}) [35]. A high reaction rate and high quantum efficiency were concurrently achieved at a high light intensity because the TiO_2-coated optical fiber bundles redistributed the total input light intensity, and thus the intensity entering each fiber was small (*ca.* 4.8×10^{12} quanta/s to 7.1×10^{13} quanta/s corresponding to the respective total input light intensities), and the decomposition reaction of isopropanol already becomes limited by mass transport when performed in this system. The distribution of photons supplied by the optical fiber that refracted into the TiO_2 coating was not uniform along the fiber length [14,22,33]. Near the input side of the fiber, the larger quantity of refracted photons (depending on TiO_2 thickness and incident light angle) means that some of the excess photons may be lost to "leaking". In contrast, at the output side of the fiber, a smaller quantity of photons is refracted to the TiO_2 coating (depending on TiO_2 thickness, fiber length, and incident light intensity), resulting in a light limit and thus decreased light utilization efficiency [35–37].

3.3. Degradation of trichloroethylene using photocatalytic optical fibers

Trichloroethylene is an organochloride compound that has been used in industries as a solvent, degreasing agent, and cleaning agent [38,39]. To effectively remove the trichloroethylene, Chen *et al.* [17] investigated the effect of photocatalysis on the degradation of trichloroethylene in the aqueous phase by a photocatalyst-coated plastic optical fiber. The TiO_2-coated plastic optical fiber

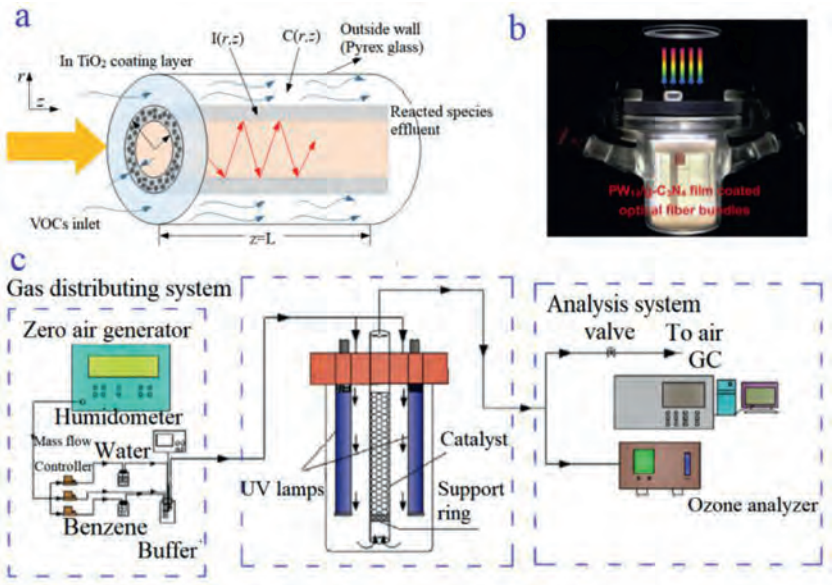

Fig. 2. (a) Schematic diagram of the optical fiber photoreactor used in a previous study. Copied with permission [25]. Copyright 2005, Young Ku. (b) Custom-made $H_3PW_{12}O_{40}$/graphitic carbon nitride film-coated optical fiber photoreactor (300 mL) for the gas-phase photocatalytic removal of aromatics. Copied with permission [31]. Copyright 2019, Elsevier. (c) Schematic diagram of the VUV photocatalytic oxidation system. Copied with permission [32]. Copyright 2017, Elsevier.

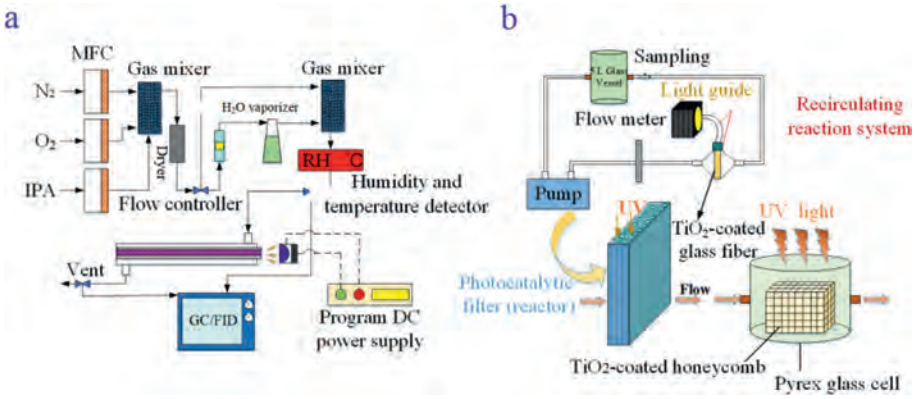

Fig. 3. (a) Schematic diagram of the tubular optical fiber photocatalytic reactor. Copied with permission [34]. Copyright 2013, Elsevier. (b) Schematic diagram of the TiO_2-coated optical-fiber-based photocatalytic reactor. Copied with permission [35]. Copyright 2000, Elsevier.

showed a higher degradation efficiency of trichloroethylene in an alkaline solution, while the ZnO-coated plastic optical fiber performed better in an acidic solution (Fig. 4a). As the thickness of the photocatalyst layer increased, the trichloroethylene degradation efficiency decreased. To determine the degradation rate, a modified Langmuir-Hinshelwood model was created as expressed by Eq. 6 [17]:

$$\frac{1}{k_{app}} = \frac{c_o}{k_{app}} + \frac{1}{k_r k_s} \tag{6}$$

where k_{app} is the apparent degradation rate constant, C_0 is the initial concentration of trichloroethylene, and k_r and k_s are the intrinsic reaction rate constant and Langmuir-Hinshelwood adsorption constant, respectively.

The parameter $R_{OH,\,UV}$ for showing the conversion efficiency of hydroxyl radicals on trichlorylethylene is calculated using Eq. 7:

$$R_{OH,UV} = \frac{\int_0^t [OH]dt}{H} = \frac{k'^D_T}{k_{OH,PCBA}} \tag{7}$$

where H is the UV fluence (mJ/cm^2), $k_{OH,\,pCBA} = 5.2 \times 10^9$ L mol^{-1} s^{-1}, and k'^D_T is the total oxidation rate constant (mJ/cm^2), which changes based on the flow rate [17]. When the pH changes in the range of 4–10, $R_{OH,\,UV}$ of ZnO-coated photocatalytic optical fibers changed more significantly than that of the fibers coated with TiO_2. Additionally, the TiO_2-coated photocatalytic optical fiber exhibited a higher trichloroethylene degradation efficiency in basic solutions, while the ZnO coating functioned better in acidic conditions.

To enhance the degradation of Trichloroethylene, TiO_2-coated plastic optical fiber bundled arrays (TiO_2-coated part length of 30 cm, 15 fibers) were employed to decompose trichloroethylene under excitation by a 1000 W xenon lamp [40]. A cylindrical plastic optical fiber bundled array reactor (650 mL; 40 cm length × 4.5 cm diameter) was manufactured, and its working principle is shown in Fig. 4b. The photocatalytic activity of photocatalyst-coated plastic optical fibers has been improved by optimizing parameters including the photocatalyst thickness, number of optical fibers, humidity, and oxygen content [41–43].

3.4. Degradation of aldehyde volatile organic compounds using photocatalytic optical fibers

Aldehyde compounds (such as formaldehyde and acetaldehyde) are recognized as typical indoor organic environmental pollutants and exist widely in modern building materials, vehicle exhaust and several food products [44]. Therefore, it is necessary to remove or degrade these toxic compounds from air.

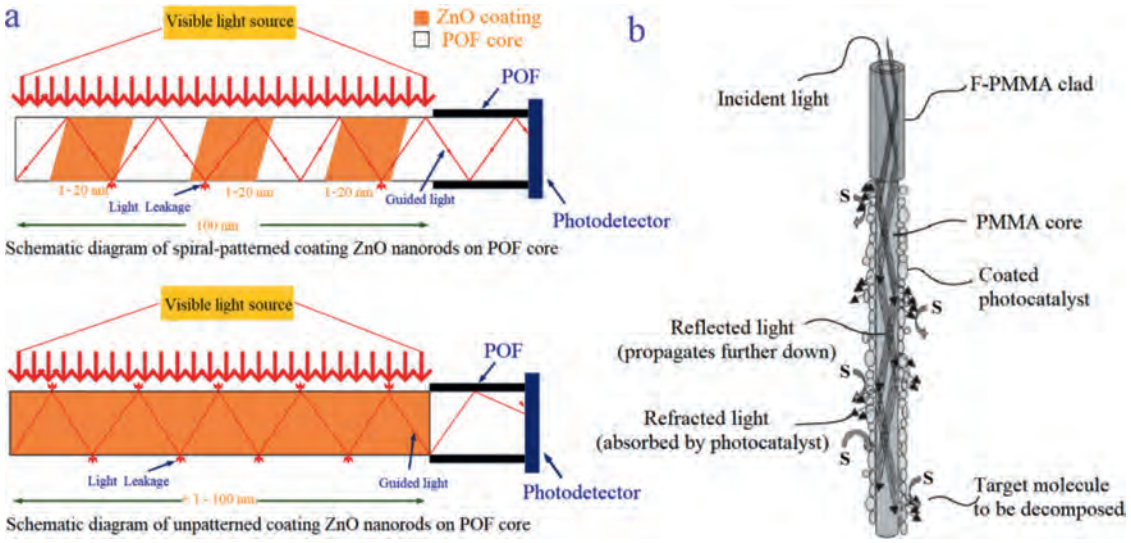

Fig. 4. (a) Schematic diagram of ZnO nanorods coated on a plastic optical fiber core. Copied with permission [75]. Copyright 2016, Waleed Soliman Mohammed. (b) Schematic diagram of photocatalytic working principle in a plastic optical fiber. Copied with permission [40]. Copyright 2003, Elsever. Abbreviations: POF, plastic optical fiber, PMMA, polymethylmethacrylate.

To remove the aldehyde organic pollutants, TiO_2-coated plastic optical fibers were explored [42]. However, the photocatalytic reactions of the organic pollutants have some limitations due to the limited length of photocatalytic plastic optical fibers and the low photonic efficiency of their coatings. To solve the limited length of TiO_2-coated plastic optical fibers, a textile was fabricated by combining a polymer (polyester), which provided robust mechanical properties, with side-emitting plastic optical fibers at a diameter of 500 μm and roughness of 10 μm [42]. The TiO_2 coating was then obtained by dipping the optical fiber textile in a concentrated aqueous suspension of TiO_2 (50 g/L) at 70 °C for 1 h and drying for 2 h at 75 °C. The TiO_2-coated textile showed a high photocatalytic efficiency for the removal of formaldehyde (degradation rate reached 76 mol h^{-1} m^{-2}) because the textile allowed for radial light leakage. As a result, the amount of light emitted on the surface of the textile from the plastic optical fibers was high, whereas diffuse light represented only approximately 2% of the total emission.

The photonic efficiency of photocatalytic coatings for the degradation of the aldehyde organic pollutants can also be improved by dispersing noble-metal nanoparticles (such as Pt, Pd, and Au) into semiconductor photocatalysts [45–48]. For example, plastic optical fibers with a Pt/TiO_2 coating showed a higher acetaldehyde oxidation rate than TiO_2-coated plastic optical fibers [45]. The metal nanoparticle dopant in the TiO_2 coating can inhibit the recombination of photogenerated electrons (e^-) and holes (h^+) and induce local surface plasmon resonance [45,49]. Furthermore, to reduce the bandgap and extend the absorption band in the visible light range, non-metal doping with carbon results in attractive photocatalytic properties since the substitution of oxygen with carbon atoms results in new energy states in the TiO_2 bandgap [50–52]. In particular, the bandgap energy of C/TiO_2 can be downregulated to 3.02 eV with 2.98% carbon [50], which can overcome the low UV transmission of plastic optical fibers. Thus, 3.2 mm thick C/TiO_2-coated plastic optical fibers showed a high photodegradation efficiency (76%) for toluene under a 500 W Hg lamp with peak wavelengths of 300, 405, and 436 nm.

3.5. Degradation of other volatile organic compounds using photocatalytic optical fibers

Methane is a greenhouse gas that is more active than carbon dioxide in the air and is widely present in natural gas, biogas, coal gas in well pits, and high-quality fuel gases. Methane in the air at a certain concentration will cause headaches, dizziness, fatigue, lack of concentration, rapid breathing and heartbeat, and other symptoms, even shock.

To remove methane in air, photocatalytic quartz optical fibers based on 110 quartz fibers (diameter of 400 μm) coated with TiO_2 (thickness of 1 mm) were adopted to degrade methane [53]. It was discovered that with a quartz optical fiber length of 20.5 cm, relative humidity of 60%, gas flow rate of 100 mL/min, and collimated UV light from a 200 W light source (mercury-xenon lamp) at wavelengths of 300–400 nm, the degradation efficiency of methane and ethylene reached 98% within 1.2 h [35]. This high degradation efficiency was attributed to the small-diameter quartz optical fibers coated with TiO_2 providing a high photoactive TiO_2 surface area. Fiber bundles were adopted because they can enhance the specific surface area and light utilization efficiency of photocatalysts [35]. In fiber bundles, to enhance the light collection capability, a long-focal-length lens in front of the fiber was employed because the receiving cone angle of the optical fiber was in the range of 8°–47°. Peill and Hoffmann [54] found that the smaller the angle of incidence is, the fewer light refractions will occur in the fiber, allowing the light to travel further along the fiber and thus making the light distribution more uniform. Once again, it has been confirmed that achieving a uniform light distribution along the optical fiber and TiO_2 coating may improve the light utilization efficiency and processing capacity of photocatalytic optical fibers.

The degradation performance of different volatile organic compounds is shown in Table 1.

4. Degradation of other gas pollutants using photocatalytic optical fibers

4.1. Degradation or conversion of CO_2 using photocatalytic optical fibers

As the main greenhouse gas, carbon dioxide severely affects the sustainability of the global ecological environment and damages human health. Methods to remove CO_2 efficiently from the atmosphere have become key to alleviating the greenhouse effect and purifying the air. Among the various measures to reduce the impact of carbon dioxide, recycling CO_2 to produce fuel is the most promising, as it could also alleviate the problems of energy shortage and environmental pollution.

Table 1
The degradation performance of different volatile organic.

Substrate	Fiber	Humidity and temperature	Light	Reactor	Performance	Ref.
Benzene	Quartz optical fibers	5% RH, 25 °C	40 W xenon arc UV, 365 nm	195 mL Pyrex glass cylindrical reactor	80% Mineralization rate in 4 h	[20]
Benzene	Fused silica fiber	30% RH, 25 °C	500 W xenon arc UV, 365 nm	20 cm-long Pyrex tubing	60% Benzene conversion in 10 min	[25]
1,2-Dichlorobenzene	Fused silica optical fibers	Room temperature	500 W UV lamp, 310–380 nm	Quartz tube (0.7 cm inner diameter, 30 cm in length)	Rate constant of 0.0182 min^{-1}	[29]
Benzene	Fused silica optical fibers	15%–25% RH, 25 °C	500 W UV lamp, 365 nm	20 cm Pyrex tubing (0.4 cm diameter)	40% Conversion in 30 min	[28]
Benzene, trichloroethylene, 2-propanol	Fused silica optical fibers	15%–25% RH	500 W UV lamp, 365 nm	20 cm Pyrex tubing (0.4 cm diameter)	40% Mineralization rate for benzene, 52% for 2-propanol, and 60% for trichloroethylene	[26]
2-Propanol	Fused silica optical fibers	Room temperature	400 W Hg-lamp, 370 nm	0.22 L Pyrex reactor	A round 9.1% conversion	[27]
Benzene, toluene, *m*-xylene	Quartz optical fibers	Ambient temperature, 73% RH	300 W Xe lamp, 320 nm	300 mL Custom-designed quartz reactor	90.3% Benzene, 100% toluene and 97.5% *m*-xylene conversions in 8 h	[31]
Isopropanol (IPA)	Fused silica optical fibers	25 °C	3 W UV-LED, 365 nm	Pyrex tubing of 200 mm length and 3 mm diameter	20% Isopropanol conversion in 30 min	[34]
Isopropanol and acetone	Quartz optical fibers	25 °C	High-pressure Hg lamp	Ceramic honeycomb monolith reactor	100% Benzene and 80% acetone conversions in 110 min	[35]
Acetone	Quartz optical fibers	30–35 °C	300 W Xe arc lamp	30 cm Stainless steel tubing	About 80% acetone removal	[46]

Photocatalysis is the most promising way to convert CO_2 to fuel. However, the overall efficiency of the photoreduction of CO_2 to fuels is mainly dependent on the use of a highly efficient catalyst [55,56] and suitable photoreactor configuration. Recently, two-phase and three-phase photocatalytic reactors have largely been used for CO_2 photoreduction, including slurries, optical fibers, and monolith reactors [19]. The electron-hole recombination rate and loss of light intensity can be reduced and the photocatalytic efficiency improved compared with traditional solid-state reactors by using optical-fiber reactors with a high specific surface area [57].

To improve the activity and stability of TiO_2-based photocatalysts for application to different photocatalytic scenarios, semiconductor coupling and doping with transition metals, noble metals, and non-metals can be performed [58]. However, doping different components can have different effects on CO_2 degradation. Under UV irradiation, it was found that the overall total energy efficiency of Cu-Fe/TiO_2-SiO_2 (0.0182%) is much higher than that on a C-Fe/TiO_2 counterpart (0.0159%) in a reactor, as shown in Fig. 5 [59]. Furthermore, the former photocatalytically reduces CO_2 to produce CH_4, whereas the latter produces C_2H_4. However, under natural light, both catalysts produced only methane with yields of 0.279 and 0.177 mol g_{cat}^{-1} h^{-1}, respectively. This phenomenon is well explained by the fact that the flat-band potential and valence band of iron oxide are lower and higher than those of TiO_2, respectively. Additionally, the presence of SiO_2 increases the efficiency of electron transfer from TiO_2 to Fe_3O_4 or CuO, while holes seem to be mainly produced by TiO_2; this inhibits electron-hole recombination and improves the photocatalytic CO_2 reduction efficiency [60]. Furthermore, previous studies have shown that Au-TiO_2 nanoparticles can selectively catalytically reduce CO_2 to CO, and a Cu-supported In_2O_3/TiO_2 photocatalyst can not only promote the conversion of CO_2 to CH_4 but also further synthesize CH_3OH [61,62].

The photocatalytic activity can be improved by doping the photocatalyst, while changing the structure of the reactor to increase contact with the gas and a uniform dispersion of light can further improve the photocatalytic CO_2 degradation efficiency [19,63–65]. In recent years, optical fiber monolith reactors with a catalyst coated on the inner surface have attracted attention due to their high light utilization ratio. Compared with the previously mentioned monolith reactors with internal irradiation, the quantum efficiency of monolith reactors with microchannels is significantly improved due to the higher luminescent surface area and increased photon-in-reactor time [66,67]. The monolith fiber reactor shown in Fig. 6 was constructed using polymethylmethacrylate optical fibers, which can transmit and scatter light to effectively illuminate the catalyst [19]. A two-dimensional simulation model was also built to better analyze the functional relationship between the quantum efficiency of photocatalytic CO_2 reduction and changes in the reactor parameters (water vapor concentration, flow rate, and light input) [68]. They found that the output methanol concentration increased with the inlet water vapor concentration and light intensity, but the methanol production efficiency decreased when the fiber deviated from the overall reactor axis. In addition, the light power reaching the reaction surface and production rate per input power were investigated to analyze the advantages of different types of monolith fiber reactors [69]. The optimum structural parameters were determined to be a middle tube radius of 1.2 mm and reactor length of 50 mm by comparing the selected parameters using monolith fiber reactors with different radii, lengths, and number of fibers. With the same velocity and fiber number, the optical power was shown to be linearly related to the photocatalytic product (methanol) concentration.

Particularly, Wang *et al.* [68] also discovered that when $KC << 1$, the kinetic rate equation for the photocatalytic reduction of CO_2 by optical fibers can be expressed as Eq. 8:

$$-r_{AS} = k_T I^n C \quad (8)$$

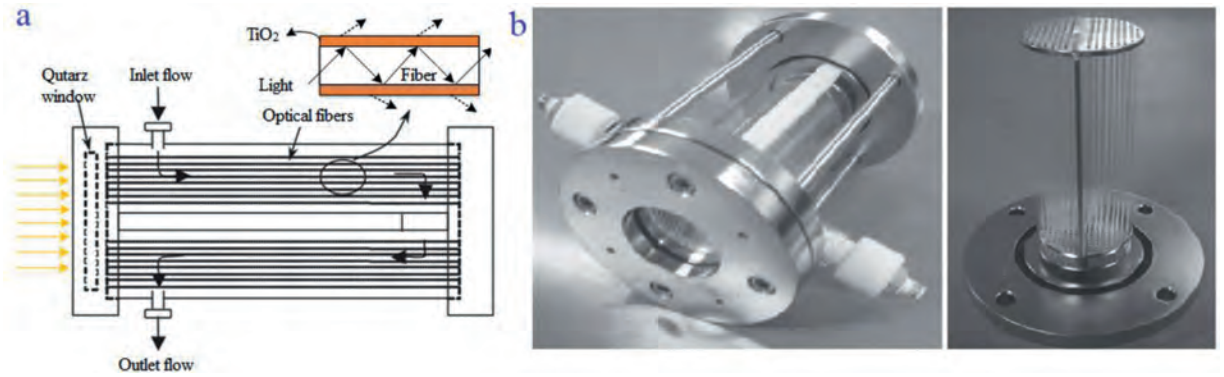

Fig. 5. (a) Schematic diagram and (b) images of a photoreactor with catalyst-coated optical fibers. Copied with permission [59]. Copyright 2008, Elsevier.

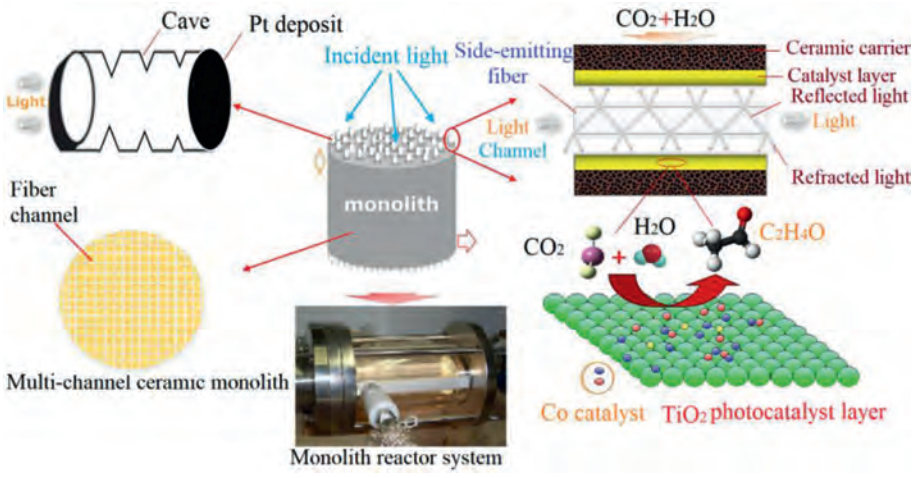

Fig. 6. Schematics of a monolith reactor and illumination fibers. Copied with permission [74]. Copyright 2010, Elsevier.

where k_T is the overall rate constant obtained by fitting the experimental data, and the index n indicates the extent of the influence of light intensity on the reaction rate, where a higher n represents a faster photocatalytic reaction. Assuming the catalyst can absorb all the light on the surface, which corresponds to n= 1, Eq. 8 can be simplified. The reaction kinetic model for the photocatalytic reduction of CO_2 to produce methanol can then be expressed as Eq. 9.

$$r = kI\frac{K_{H_2O}K_{CO_2}(P_{H_2O}P_{CO_2})}{(1+K_{H_2O}P_{H_2O}+K_{CO_2}P_{CO_2}+K_{CH_3OH}P_{CH_3OH})^2} \quad (9)$$

4.2. Degradation of ammonia, nitric oxide (NO) and hydrogen sulfide (H_2S) using photocatalytic optical fibers

Aammonia, NO and H_2S are gaseous pollutants present in daily life that are produced in various industries such as medicine and agriculture [70]. Ammonia gas, which is mainly produced by agricultural and animal husbandry activities, will burn the mucous membranes of the skin, eyes, and respiratory organs. NO is largely produced by transportation and fuel combustion and may cause water, soil, and atmospheric pollution. Inhaling a certain amount of these gases can damage the respiratory tract [71] and cause lung swelling, headaches, dizziness, and other symptoms [72]. H_2S is identified as a gasotransmitter and is colorless, odorous, and highly toxic, which could be found in air and causes acidic rain and corrosion.

Ammonia gas and NO can be removed by intimately coupling photocatalysis and quartz optical fibers. The performance of photocatalytic optical fibers is tied to the influence of the catalyst. Improving the coating method and doping can effectively improve the reaction efficiency. In one study, the TiO_2 coatings were prepared by three different methods (thermal hydrolysis, Hombikat XXS100, and P25) to improve quartz optical fibers (300–400 nm, 70 W light/matt) for ammonia gas degradation [53]. Compared with Hombikat XXS100 and P25, the thermal hydrolysis coating reduced the surface contact angle to nearly zero more quickly under UV light, showed super hydrophilicity, and recovered the contact angle slower after the lamp was turned off. Therefore, the thermal hydrolysis coating could more effectively react with water to generate ·OH radicals and carry out the reduction reaction. The thermal hydrolysis coating not only has a strong photoactivity but is also smooth and resistant to cracking, and so this method is suitable for the preparation of TiO_2 films.

Of natural light, the UV range accounts for only 5%, and since pure TiO_2 (wide bandgap of 3.2 eV) is only excited by UV light, the utilization efficiency of natural light is limited. Coating Ag/TiO_2, Cu/TiO_2, Pt/TiO_2, or other metal-doped TiO_2 on quartz optical fibers has thus been explored to degrade NO (50/400 ppm). These doped coatings make the redox reaction more effective by extending the excitation band of TiO_2 to the visible light region (wavelengths > 380 nm) and allowing for more efficient light utilization. For oxygen/water vapor, the material with the lowest activity in the UV-visible spectrum is Cu/TiO_2, and that with the highest activity is Pt/TiO_2, the degradation efficiency of which can reach 90% [73]. Therefore, in future research, it is particularly important to rationally design and optimize the TiO_2-coated quartz optical fiber parameters (incident light intensity and angle; fiber length, diameter, and number; catalyst coating thickness; *etc.*) and determine how to apply photocatalysts to improve their quantum and

light utilization efficiencies toward improving the photocatalytic efficiency. In particular, achieving a uniform distribution of light along the fiber and TiO_2 coating may be a good choice to improve the light utility and processing capacity.

Furthermore, in the process of using optical fiber photocatalysis to degrade H_2S, Brancher *et al.* [16] employed the mass balance equation for a steady-state plug flow reactor and obtained the following Eq. 10:

$$\frac{V}{Q} = \frac{1}{kK}(C_{inlet}/C_{outlet}) + \frac{1}{k}(C_{inlet} - C_{outlet}) \quad (10)$$

where Q is the volumetric gas flow rate, the ratio V/Q represents the average time for molecules to pass through the optical reactor, and C_{outlet} and C_{inlet} are the pollutant concentration at the reactor outlet and inlet, respectively. After simplification, the above formula can be written as follows (Eq. 11):

$$\frac{\ln(C_{inlet}/C_{outlet})}{C_{inlet} - C_{outlet}} = \frac{kK\tau}{C_{inlet} - C_{outlet}} - K \quad (11)$$

Through the constructed kinetic model for the photocatalytic oxidation of H_2S based on the Langmuir-Hinshelwood approach, the reaction constant (k) was calculated as approximately 10.5 μmol m^{-3} s^{-1} and the adsorption constant (K) as 5263 m^{-3}.

5. Conclusion and future prospects

In this review, we systematically covered developments in photocatalytic optical fibers for the degradation and conversion of air pollutants. The principle of optical fiber photocatalysis for representative photocatalytic optical fibers was summarized, and we highlighted the reported effects of the structural parameters of photocatalytic optical fibers on their photocatalytic and quantum efficiencies. Moreover, the Langmuir-Hinshelwood kinetic rate equation was summarized to analyze the photocatalytic reduction of gaseous pollutants, which provides important information for the design of effective methods to improve the performance of photocatalytic fibers toward the removal and conversion of gaseous pollutants.

To use photocatalytic optical fibers for the rapid and sustainable degradation and conversion of air pollutants, the performance of the optical fibers should be further enhanced. The excitation light intensity of the photocatalyst coating on the optical fibers is affected by incident light angle, fiber length, fiber diameter, fiber number, catalyst coating thickness, *etc.* Importantly, the photocatalytic optical hollow-fibers, which RI of the fiber (air) core (n_{co}) is lower than that of the fiber cladding (n_{cl}) and RI of the n_{cl} is lower than that of the photocatalyst coating, should be adopted to enhance the excitation light intensity of the photocatalyst coating for the degradation and conversion of air pollutants.

The photocatalyst activity is also an important factor affecting the degradation or conversion of gaseous pollutants by optical fibers. As such, the doping of well-known semiconductors such as TiO_2 and ZnO with upconversion luminescent metals, metal oxides, or non-metals such as carbon or carbon nitrides, as well as the use of composites and perovskite-based materials, would be another way to improve the degradation and conversion efficiencies for air pollutants. In particular, accurate matching between the photocatalyst and oxidation or reduction required for the degradation and conversion of air pollutants is very important, because photocatalysts include strong oxidation photocatalysts and reduction photocatalysts. The photocatalytic optical fibers with strong oxidation photocatalysts can easily remove gaseous organic pollutants and NO, and the photocatalytic optical fiber with strong reducibility is a good choice for CO_2 conversion. The Langmuir-Hinshelwood model can be used to analyze the optimal photocatalytic reaction conditions, and thus increases the efficiency of photocatalytic removal of toxic gases. Furthermore, the porous structure of photocatalytic coatings and their ability to adsorb reactants and desorb products also need further improvement. Therefore, many challenges and questions remain to be addressed in the use of optical fibers to degrade and convert air pollutants.

Declaration of competing interest

The authors declare that they have no known competing financial interests or personal relationships that could have appeared to influence the work reported in this paper.

Acknowledgments

The authors gratefully acknowledg support from the National Natural Science Foundation of China (NSFC) (Nos. 51876018 and 52176178), the Innovation research group of universities in Chongqing (No. CXQT21035), the Postgraduate Research Innovation Project of Chongqing University of Technology (No. ycx20192047), the Postgraduate Research Innovation Project of Chongqing (Nos. CYS18309 and CYS19318) and the Science and Technology Research Project of Chongqing Education Commission (No. KJQN201801126).

References

[1] W.W. Li, H.Q. Yu, B.E. Rittmann, Nature 528 (2015) 29–31.
[2] N. Madima, S.B. Mishra, I. Inamuddin, A.K. Mishra, Environ. Chem. Lett. 18 (2020) 1169–1191.
[3] N.B. Zhong, J.L. Yuan, Y.H. Luo, et al., Chem. Eng. J. 425 (2021) 130666.
[4] Y.W. Wu, L.L. Zhong, J.L. Yuan, et al., Environ. Chem. Lett. 19 (2020) 1335–1346.
[5] B. Karimi, C. Meyer, D. Gilbert, N. Bernard, Environ. Chem. Lett. 14 (2016) 467–475.
[6] P.J. Landrigan, R. Fuller, N.J.R. Acosta, et al., Lancet 391 (2018) 10119.
[7] A. Luengas, A. Barona, C. Hor, et al., Rev. Environ. Sci. Bio. 14 (2015) 499–522.
[8] K. Zhao, X. Sun, C. Wang, et al., Chin. Chem. Lett. 32 (2021) 2963–2974.
[9] T.L. Xia, Y.C. Lin, W.Z. Li, M.T. Ju, Chin. Chem. Lett. 32 (2021) 2975–2984.
[10] G.S. Shi, A. Mahmood, G. Lu, et al., Catal. Lett. 149 (2019) 2728–2738.
[11] M.Y. Wu, D.Y.C. Leung, Y.G. Zhang, et al., Chem. Eng. Sci. 195 (2019) 985–994.
[12] Z. Shayegan, C.S. Lee, F. Haghighat, Chem. Eng. J. 334 (2018) 2408–2439.
[13] S. Joks, M. Krichevskaya, S. Preis, Catal. Lett. 141 (2011) 309–315.
[14] R.E. Marinangeli, D.F. Ollis, AIChE J. 23 (1977) 415–426.
[15] K. Hofstadler, R. Bauer, S. Novalic, G. Heisler, Environ. Sci. Technol. 28 (1994) 670–674.
[16] M. Brancher, D. Franco, H. de Melo Lisboa, Environ. Technol. 37 (2016) 2852–2864.
[17] C.J. Chen, C.C. Wu, L.T. Hsieh, K.C. Chen, Water 11 (2019) 2391 (Basel).
[18] A. Danion, J. Disdier, C. Guillard, F. Abdelmalek, N. Jaffrezic-Renault, Appl. Catal. B Environ. 52 (2004) 213–223.
[19] P.Y. Liou, S.C. Chen, J.C.S. Wu, et al., Environ. Sci. Technol. 4 (2011) 1487–1494.
[20] W. Wang, Y. Ku, J. Photochem. Photobiol. A 159 (2003) 47–59.
[21] N.B. Zhong, M. Chen, Y.H. Luo, et al., Chem. Eng. J. 355 (2019) 731–739.
[22] R.E. Marinangeli, D.F. Ollis, AIChE J. 26 (1980) 1000–1008.
[23] P. Wyness, J.F. Klausner, D.Y. Goswami, K.S. Schanze, J. Sol. Energy Eng. 116 (1994) 2–7.
[24] C.M. Ma, W. Wang, Y. Ku, F.T. Jeng, Chem. Eng. Technol. 1 (2007) 1083–1087.
[25] W. Wang, Y. Ku, C.M. Ma, F.T. Jeng, J. Appl. Electrochem. 35 (2005) 709–714.
[26] C.M. Ma, Y. Ku, Y.C. Chou, F.T. Jeng, J. Environ. Eng. Manag. 18 (2008) 363–369.
[27] S. Hager, R. Bauer, Chemosphere 38 (1999) 1549–1559.
[28] C.M. Ma, Y. Ku, Y.C. Chou, F.T. Jeng, J. Environ. Eng. Manag. 18 (2008) 363–369.
[29] M. Ren, K.T. Valsaraj, Sep. Purif. Technol. 62 (2008) 523–528.
[30] J.I.L. Chen, G. von Freymann, V. Kitaev, G.A. Ozin, J. Am. Chem. Soc. 129 (2007) 1196–1202.
[31] J.Q. Meng, X.Y. Wang, X. Yang, et al., Appl. Catal. B: Environ. 251 (2019) 168–180.
[32] J. Ji, Y. Xu, H.B. Huang, et al., Chem. Eng. J. 327 (2017) 490–499.
[33] W. Choi, J.Y. Ko, H. Park, J.S. Chung, Appl. Catal. B: Environ. 31 (2001) 209–220.
[34] W.M. Hou, Y. Ku, J. Mol. Catal. A Chem. 374 (2013) 7–11.
[35] R.D. Sun, A. Nakajima, L. Watanabe, T. Watanabe, K. Hashimoto, J. Photochem. Photobiol. A 136 (2000) 111–116.
[36] N.J. Peill, M.R. Hoffmann, Environ. Sci. Technol. 29 (1995) 2974–2981.
[37] N.J. Peill, M.R. Hoffmann, Environ. Sci. Technol. 30 (1996) 2806–2812.
[38] S. Yamazaki, S. Matsunaga, K. Hori, Water Res. 35 (2001) 1022–1028.
[39] M. Keshmiri, M. Mohseni, T. Troczynski, App. Catal. B: Environ. 53 (2004) 209–219.
[40] H. Joo, H. Jeong, M. Jeon, I.I. Moon, Sol. Energy Mater. Sol. Cells 79 (2003) 93–101.
[41] A. Danion, J. Disdier, C. Guillard, F. Abdelmalek, N. Jaffrezic-Renault, Int. J. Appl. Electrom. 23 (2006) 187–201.

[42] P.A. Bourgeois, E. Puzenat, L. Peruchon, et al., Appl. Catal. B: Environ. 128 (2012) 171–178.
[43] A. Danion, J. Disdier, C. Guillard, O. Païsséc, N. Jaffrezic-Renaulta, Appl. Catal. B: Environ. 62 (2006) 274–281.
[44] Y. Huang, S.S.H. Ho, Y. Lu, et al., Molecules 21 (2016) 56.
[45] A.J. Anceno, R.M. Stuetz, Appl. Catal. B: Environ. 181 (2016) 661–671.
[46] Y. Choi, M.S. Koo, A.D. Bokare, et al., Environ. Sci. Technol. 51 (2017) 3973–3981.
[47] V. Vaiano, G. Lervolino, D. Sannino, et al., Appl. Catal. B: Environ. 188 (2016) 134–146.
[48] Y.L. Zhao, Y.C. Wei, X.X. Wu, et al., Appl. Catal. B: Environ. 226 (2018) 360–372.
[49] S. Linic, P. Christopher, D.B. Ingram, Nat. Mater. 10 (2011) 911–921.
[50] M.S. Kim, G. Liu, W.K. Nam, B.W. Kim, J. Ind. Eng. Chem. 17 (2011) 223–228.
[51] T. Fotiou, T.M. Triantis, T. Kaloudis, et al., Water Res. 90 (2016) 52–61.
[52] Y.W. Wu, W.H. Xiang, L.Y. Li, et al., Chem. Eng. J. 420 (2021) 130517.
[53] A. Gonzalez-Martin, A.S. Jeevarajan, O.J. Murphy, J. Adv. Oxid. Technol. 3 (1998) 253–260.
[54] N.J. Peill, M.R. Hoffmann, Environ. Sci. Technol. 29 (1995) 2974–2981.
[55] T.M. Su, Z.Z. Qin, H.B. Ji, Y.X. Jiang, G. Huang, Environ. Chem. Lett. 14 (2016) 99–112.
[56] A.A. Khan, M. Tahir, J. CO_2 Util. 29 (2019) 205–239.
[57] J.C.S. Wu, T.H. Wu, T. Chu, H. Huang, D. Tsai, Top. Catal. 47 (2008) 131–136.
[58] Y. Boyjoo, H.Q. Sun, J. Liu, V.K. Pareek, S.B. Wang, Chem. Eng. J. 310 (2017) 537–559.
[59] T.V. Nguyen, J.C.S. Wu, Sol. Energy Mater. Sol. Cells 92 (2008) 864–887.
[60] T.V. Nguyen, J.C.S. Wu, Appl. Catal. A: Gen. 335 (2008) 112–120.
[61] M. Tahir, B. Tahir, N.A.S. Amin, H. Alias, Appl. Surf. Sci. 389 (2016) 46–55.
[62] M. Tahir, N.A.S. Amin, Int. J. Hydrog. Energy 42 (2017) 15507–15522.
[63] J.C.S. Wu, Catal. Surv. Asia 13 (2009) 30–40.
[64] J.C.S. Wu, H.M. Lin, C.L. Lai, Appl. Catal. A: Gen. 296 (2005) 194–200.
[65] O. Ola, M. Maroto-Valer, D. Liu, et al., Appl. Catal. B: Environ. 126 (2012) 172–179.
[66] M. Tahir, N.A.S. Amin, Appl. Catal. A: Gen. 467 (2013) 483–496.
[67] M. Tahir, B. Tahir, Z.Y. Zakaria, A. Muhammad, J. Clean. Prod. 213 (2019) 451–461.
[68] T.C. Wang, L.J. Yang, X.Z. Du, Y.P. Yang, Energy Convers. Manag. 65 (2013) 299–307.
[69] K. Yuan, L.J. Yang, X.Z. Du, Y.P. Yang, Energy Convers. Manag. 87 (2014) 258–266.
[70] M.S. Kamal, S.A. Razzak, M.M. Hossain, Atmos. Environ. 140 (2016) 117–134.
[71] R. Sun, C. He, L. Fu, et al., Chin. Chem. Lett. 33 (2022) 527–532.
[72] R.M. Heck, Catal. Today 53 (1999) 519–523.
[73] Y.H. Yu, I.H. Su, J.C.S. Wu, Environ. Technol. 31 (2010) 1449–1458.
[74] Y.W. Zhen, H.C. Chou, J.C.S. Wu, P. Din, G. Mul, Appl. Catal. A: Gen. 380 (2010) 172–177.
[75] H.R.B.A. Rahim, M.Q.B. Lokman, S.W. Harun, et al., J. Nanophotonics 10 (2016) 036009.